

# RSC Advances



This is an *Accepted Manuscript*, which has been through the Royal Society of Chemistry peer review process and has been accepted for publication.

*Accepted Manuscripts* are published online shortly after acceptance, before technical editing, formatting and proof reading. Using this free service, authors can make their results available to the community, in citable form, before we publish the edited article. This *Accepted Manuscript* will be replaced by the edited, formatted and paginated article as soon as this is available.

You can find more information about *Accepted Manuscripts* in the [Information for Authors](#).

Please note that technical editing may introduce minor changes to the text and/or graphics, which may alter content. The journal's standard [Terms & Conditions](#) and the [Ethical guidelines](#) still apply. In no event shall the Royal Society of Chemistry be held responsible for any errors or omissions in this *Accepted Manuscript* or any consequences arising from the use of any information it contains.

1 **Insights into the enhancement mechanism coupling with adapted adsorption**  
2 **behavior from mineralogical aspect in bioleaching of copper-bearing sulfide ore by**  
3 ***Acidithiobacillus* sp.**

4

5 Shoushuai Feng, Hailin Yang\* and Wu Wang

6

7

8

9 S. Feng • H. Yang (✉) • W. Wang

10 The Key Laboratory of Industrial Biotechnology, Ministry of Education, School of Biotechnology,

11 Jiangnan University, 1800 Lihu Road, Wuxi, 214122. People's Republic of China.

12 Tel: +86 85913671.

13 Fax: +86 85918119.

14 \* e-mail: fengss@jiangnan.edu. cn

15

16

17

18

19

20

21

22

23

24

25

26

## 27 Abstract

28 The enhancement mechanism of adapted adsorption behavior in bioleaching of copper-bearing sulfide ore  
29 by *Acidithiobacillus* sp. was systematically investigated from a mineralogical aspect and compared to  
30 adsorption-deficient (DF) and adsorption-unadapted (UA) systems. With the assistance of adapted  
31 adsorption behavior, both iron and sulfur metabolism was enhanced, which was proved by a series analysis  
32 of key chemical parameters, including scanning electron microscopy (SEM) and X-ray diffraction (XRD).  
33 SEM analysis revealed smaller jarosite and S<sup>0</sup> granules along with more potential adsorption sites on the  
34 ore surface, thus indicating a stronger “contact” mechanism. XRD analysis showed that more chemical  
35 derivatives were generated owing to active iron/sulfur metabolism. Additionally, attached and free  
36 biomasses of *A. ferrooxidans* and *A. thiooxidans* were increased by 33.3%-58.9% and 25.0%-33.9%,  
37 respectively. Moreover, the final concentration of extracted copper ion was improved by 22.8% (*A.*  
38 *ferrooxidans*) and 28.9% (*A. thiooxidans*), respectively. All results proved that the adsorption behavior  
39 coupled to attached cells was greatly stimulated and accelerated by the adapted evolution and further  
40 contributed to higher bioleaching efficiency. The adapted method and its mechanism will be useful to  
41 further guide similar bioleaching processes in the near future.

42 **Keywords:** Bioleaching of copper-bearing sulfides ore · *Acidithiobacillus* · Adapted adsorption  
43 behavior · Mineralogical enhancement mechanism

## 44 1. Introduction

45 A vast majority of low-grade ores cannot be economically utilized by the traditional smelting method  
46 and are deposited at mines.<sup>1-3</sup> The substantial discard of ores are accumulating, resulting in resource waste  
47 and potential environmental problems. The copper-bearing sulfide ore such as chalcopyrite (CuFeS<sub>2</sub>),  
48 (>70% of world copper reserves), is general common low-grade and refractory that also faces the  
49 aforementioned problems.<sup>4,5</sup> In the last decades, bioleaching was recognized as a green and economical  
50 technology for recovering these waste ores.<sup>6-8</sup> However, owing to the complicated and refractory structure,  
51 the commercial application of bioleaching of copper-bearing sulfide ore is still not satisfactory.<sup>9,10</sup> Recently,  
52 bioleaching of copper-bearing sulfide ore has attracted increasing attentions, especially because of the  
53 growing copper consumption and environmental stress worldwide.

54 To improve bioleaching process, it is essential to deep understand the bioleaching mechanism in detail.  
55 Various mechanisms have been proposed for illustrate the bioleaching process of sulfide ore (pyrite,  
56 sphalerite, chalcopyrite etc.), such as surface attaching, oxidation reactions, elemental transformation,  
57 interfacial evolution, bio-molecules changes, and surface erosions.<sup>11</sup> Two indirect mechanisms via  
58 thiosulfate or via polysulfides were found in pyrite bioleaching with *A. thiooxidans*.<sup>12</sup> The sphalerite  
59 bioleaching process was divided into two steps.<sup>13</sup> The rapid surface attaching of microorganisms was the  
60 key to enhance leaching efficacy, resulting in the oxidation of the pyrite and concomitant bio-generation of  
61 ferric ions and protons. Then, the continued regeneration of ferric ions by planktonic bacteria and the  
62 oxidation of the elemental sulfur reaction product further contributed the higher leaching efficacy.  
63 Currently, “indirect contact” and “direct contact” mechanisms were proposed to better understand the  
64 bioleaching process.<sup>14,15</sup> The two mechanisms derived from bio-oxidation reactions from different spaces.  
65 In the former mechanism, bacteria oxidize soluble ferrous ion to ferric ion and sulfur to sulfate ion in the  
66 micro-liquid environment. Ferric ions oxidize the sulfide ore in an acidic environment. In the latter  
67 mechanism, bacterial attachment is important physiologically, but ferric ions oxidize the sulfide minerals in  
68 the solid-liquid interface environment. The specifics of bacterial (electro) chemical interactions with  
69 mineral surfaces and/or their direct contact (enzymatic) contribution to sulfide dissolution are unknown. In  
70 these mechanisms, the adsorption behavior of attached cell was prerequisite for the subsequent iron/sulfur  
71 metabolism.<sup>16</sup> Previous researches have also intensively studied the performance of adsorption behavior,  
72 such as the effect of single factor such as extracellular polymeric substance (EPS), mineral or bacterial  
73 attachment selection in various bioleaching processes.<sup>16,17</sup> It was reported that a multilayered biofilm  
74 around with EPS of *A. ferrooxidans*, *A. thiooxidans* and *Leptospirillum ferrooxidans* was pivotal in  
75 “contact” mechanisms.<sup>18,19</sup> The attached behaviors of different strains even with closely related  
76 genetic relationship were diverse, while the mineral-selection in the attached process of the same strain was  
77 also different.<sup>14,20</sup> However, most researchers focused on the adsorption kinetics, association factor and  
78 adsorption characteristics between different species. To date, to the best of our knowledge, the detailed  
79 mechanism of adsorption behavior in bioleaching of copper-bearing sulfide ore, especially the efficient  
80 strategy for enhancing the performance of adsorption behavior remains poorly understood.

81 In our previous study, an acidophilic strain *A. thiooxidans* ZJJN-3 was isolated from industrial bio-heap

82 leachate.<sup>21</sup> *A. thiooxidans* ZJJN-3 and *A. ferrooxidans* CUMT-1 was applied in chalcopyrite bioleaching to  
83 form an efficient catalytic system.<sup>22</sup> An integrated fermentation strategy was also proposed for enhancing  
84 chalcopyrite bioleaching in a 7-L bioreactor.<sup>23</sup> In this study, the typical bioleaching strains (*A. ferrooxidans*  
85 and *A. thiooxidans*) were employed for exploring the enhancement mechanism of adapted adsorption  
86 behavior in bioleaching of copper-bearing sulfide ore. First, the effects of adapted adsorption behavior on  
87 sulfur and iron metabolism were analyzed and compared to adsorption-deficient (DF) and  
88 adsorption-unadapted (UA) systems. Second, the effects of adaptive adsorption behavior on ore such as  
89 morphological, componential and functional group differences were also investigated by scanning electron  
90 microscopy (SEM), and X-ray diffraction (XRD), respectively. Finally, the efficiency of adaptive  
91 adsorption behavior on improving cell growth and bioleaching efficiency was further verified.

## 92 2. Materials and methods

### 93 2.1. Strain and growth condition

#### 94 (Position for Table 1)

95 *A. ferrooxidans* CUMT-1 was kindly donated by Professor Leng from the China University of Mining  
96 and Technology, Xuzhou, Jiangsu, China. *A. thiooxidans* ZJJN-3 was isolated from leachate of industrial  
97 bio-heap (low-grade secondary sulfide, 20 million m<sup>3</sup>) in Zijinshan Copper Mine, Longyan, Fujian, China.  
98 The strain was previously identified by analysis of physiological and molecular characteristics.<sup>21</sup> It was  
99 deposited in the China Center for Type Culture Collection with the number M2012104. The detailed strain  
100 characteristics are listed in Table 1. *A. ferrooxidans* was cultured in 9K media and *A. thiooxidans* was  
101 cultured in Starkey media. The basal salts of 9K media were listed as follows (g/L): (NH<sub>4</sub>)<sub>2</sub>SO<sub>4</sub> 3.0,  
102 K<sub>2</sub>HPO<sub>4</sub> 0.5, MgSO<sub>4</sub>·7H<sub>2</sub>O 0.5, KCl 0.1, Ca(NO<sub>3</sub>)<sub>2</sub> 0.01. Energy substrate: 44.7 g/L FeSO<sub>4</sub>·7H<sub>2</sub>O. The  
103 basal salts of Starkey media were listed as follows (g/L): (NH<sub>4</sub>)<sub>2</sub>SO<sub>4</sub> 3.0, KH<sub>2</sub>PO<sub>4</sub> 3.5, MgSO<sub>4</sub> 0.5,  
104 CaCl<sub>2</sub>·2H<sub>2</sub>O 0.25. Energy substrate: 10 g/L S<sup>0</sup>. Trace elements were listed as follows (mg/L): Na<sub>2</sub>SO<sub>4</sub> 50.0,  
105 FeCl<sub>3</sub>·6H<sub>2</sub>O 11.0, H<sub>3</sub>BO<sub>3</sub> 2.0, MnSO<sub>4</sub>·H<sub>2</sub>O 2.0, ZnSO<sub>4</sub>·7H<sub>2</sub>O 0.9, Na<sub>2</sub>MoO<sub>4</sub>·2H<sub>2</sub>O 0.8, CoCl<sub>2</sub>·6H<sub>2</sub>O 0.6,  
106 CuSO<sub>4</sub> 0.5, Na<sub>2</sub>SeO<sub>4</sub> 0.1. For both bacetrail systems, the initial pH of the media was adjusted to 2.2 and the  
107 strains were adapted by 3.0% (w/v) of copper-bearing sulfide ore sample at 30 °C and 170 rpm. Strains  
108 were incubated into fresh media once a month.

109 *2.2. Ore sample composition and pretreatment*

110 **(Position for Table 2)**

111 The copper-bearing sulfide ore sample was collected from Dongguashan copper mine, Tongling, Anhui,  
112 China. The main mineralogical compositions of the primary ore were chalcopyrite, pyrite, pyrrhotite,  
113 and magnetite. The detailed elements and contents of the ore sample were assayed by atomic absorption  
114 spectrometry (Spectr AA-220, Varian, USA) as Table 2. The ore sample was sieved through a 300-mesh  
115 grid, with controlling particle diameter <48  $\mu\text{m}$ . The ore sample was sequentially washed with 2 M HCl,  
116 distilled water, and pure ethanol. Then, the ore sample was dried at room temperature and reserved in a  
117 vacuum desiccator.

118 *2.3. Experimental procedure*

119 *2.3.1. Procedure for DF system*

120 The DF system was designed as described here. The leaching solution was allowed to rest without  
121 agitation for 1 h to allow the ore particles to settle. Then, supernatant was transferred into another flask.  
122 The leached ore sample was collected by centrifugation (3K15, Sigma, Germany) at  $380 \times g$  for 2 min. The  
123 ore sample was suspended in 30 mL of fresh basal salts of 9K or Starkey media. Then 1.0 g of 0.2 mm  
124 glass beads was added and shaken with a vortex (lab-dancer, IKA, Germany) for 5 min. The ore sample  
125 was centrifuged and shaken again. The supernatant was then transferred into another tube. Almost no  
126 dissociative DNA was tested in the supernatant by this method according to the report of Gehrke et al.  
127 (1998), indicating that all attached cells were removed without breaking.<sup>24</sup> Moreover, no additional cells  
128 were separated with an additional shaken-operation process, proving that all attached cells were separated  
129 from the ore surface with the above operation. The ore sample was added into its original bioleaching  
130 supernatant. The above procedure was completed every five days.

131 *2.3.2. Procedure of adsorption-adapted (AD) evolution*

132 The AD evolution was processed as described as here. *A. ferrooxidans* and *A. thiooxidans* were  
133 independently cultured with 3.0% (w/v) of copper-bearing sulfide ore for 15 days. The leaching solution  
134 was still for 1 h and the supernatant was transferred into another flask. The ore sample was collected by  
135 centrifugation (3K15, Sigma, Germany) at  $380 \times g$  for 2 min, and suspended in 30 mL of fresh basal salts

136 of 9K or Starkey media. Then, 1.0 g of 0.2-mm glass beads was added and shaken with a vortex (lab-dancer,  
137 IKA, Germany) for 5 min. Most of the attached cells with poor adsorption performance were washed off  
138 while stronger ones were preserved. The ore sample was centrifuged, as before, and added into fresh media.  
139 This above process was repeated once every two weeks. After being repeated for 6 months, the attached  
140 cells were shed and collected, as in 2.3.1. The attached cells were used as the adapted strain for the  
141 bioleaching experiment.

### 142 2.3.3. Bioleaching experiment

143 Six bioleaching experiments with different performances of adsorption behavior were designed as  
144 follows: *A. ferrooxidans* CUMT-1 (DF); *A. ferrooxidans* CUMT-1 (unadapted; UA); *A. ferrooxidans*  
145 CUMT-1 (AD); *A. thiooxidans* ZJJN-3 (DF); *A. thiooxidans* ZJJN-3 (UA); *A. thiooxidans* ZJJN-3 (AD).  
146 The bioleaching experiments were carried out in 500-mL shaker flasks; 100 mL media was added into the  
147 *A. ferrooxidans* (9K basal salts media) and *A. thiooxidans* (Starkey basal salts media) systems. Then, 3.0 g  
148 of copper-bearing sulfide ore sample was added into each flask. The cell density in each system was  
149 controlled at  $5.0 \times 10^7$  cells/mL after inoculation. The bioleaching experiments were carried out at 30 °C  
150 and 170 rpm. To balance the system from evaporation loss, 2.0 mL of sterile water was supplemented into  
151 each system once a day. The whole bioleaching cycle lasted 40 days.

## 152 2.4. Analytical methods

### 153 2.4.1. pH and Eh measurement

154 The pH value was measured by a pH meter (PHB-3TC, Sartorius, Germany). The Eh value was  
155 monitored by a Pt electrode (E-431Q, ASI, USA) with a calomel electrode (Hg/Hg<sub>2</sub>Cl<sub>2</sub>) as reference.

### 156 2.4.2. Sulfate ion assay

157 The concentration of sulfate ions was detected according to the chromic acid-barium colorimetric assay  
158 using a spectrophotometer (IV-1100D, Meipuda, China). Concentration of sulfate ion (mg/L) =  $201.6 \times$   
159  $OD_{420\text{ nm}} - 26.029$  ( $r^2=0.998$ ).

### 160 2.4.3. Ferrous and ferric ion assay

161 The concentrations of ferrous and ferric ions were measured according to the *o*-phenanthroline  
162 spectrophotometry assay using a spectrophotometer. Concentration of ferrous ion (mg/L) =  $5.077 \times OD_{508}$

163  $\text{nm} - 0.0765$  ( $r^2=0.999$ ). Concentration of ferric ion (mg/L) =  $5.102 \times \text{OD}_{508 \text{ nm}} - 0.143$  ( $r^2=0.998$ ).

#### 164 2.4.4. SEM analysis

165 The ore sample was previously dried at room temperature and preserved in a vacuum desiccator. The  
166 morphology and surface of the ore were observed with an SEM (Quanta-200, FEI, Netherlands). The  
167 suspension solution of ore sample was added at specimen holder. After the natural volatilization, the  
168 sample was firmly immobilized and a 30 nm thick conductive coating of gold was applied to the surface.  
169 The scanned condition was set at 25 kV.

#### 170 2.4.5. XRD analysis

171 The ore sample was previously washed with deionized water and dried at room temperature under the  
172 vacuum condition. Then the ore was covered on the center depression of the detection plate. The ore  
173 sample was scanned according to 2-Theta range 3-90 ( $^\circ$ ) by an X-ray diffractometer (D8, AXS, Germany).  
174 The detailed data were analyzed by the MDI Jade 5.0 (Materials Data Ltd., USA) integrating PDF card  
175 library.

#### 176 2.4.6. Detection of free, attached and total cell density

177 One milliliter of bioleaching sample was centrifuged at  $380 \times g$  for 2 min to separate the supernatant  
178 from the ore precipitation. The free cell density was counted by a single span microscope. Meanwhile, the  
179 bottom ore sample was re-suspended in 5.0 mL of fresh basal media. Then, 0.2 g of 0.2-mm glass beads  
180 were added and shaken with a vortex for 5 min. This sample was centrifuged and the mixing process was  
181 repeated once. The attached cell density was counted in the supernatant as before. The total cell density was  
182 the sum of the free and attached cell densities.

#### 183 2.4.7. Copper ion assay

184 The concentration of copper ion was monitored by flame atomic absorption spectrometry (Spectr  
185 AA-220, Varian, USA). Concentration of copper ion (mg/L) =  $6.852 \times \lambda_{325 \text{ nm}} - 0.0301$  ( $r^2=0.999$ ).

#### 186 2.5. Statistical analysis

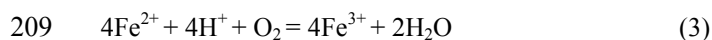
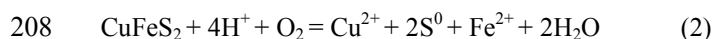
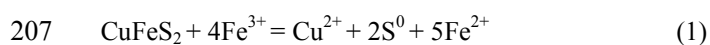
187 All experiments were performed in triplicate. The statistical analysis of experimental data was  
188 performed by one-way analysis of variance and expressed as mean values  $\pm$  SD. The software SPSS 17.0  
189 (SPSS Inc., Chicago, USA) was used for the statistical analysis.

### 190 3. Results and discussion

#### 191 3.1. Effects of adapted adsorption behavior on iron and sulfur metabolisms

##### 192 3.1.1. Iron metabolism

193 Changes in ferrous and ferric ions, the main parameters of iron metabolism, in different systems are  
194 shown in Fig. 1. The main biochemical reactions in copper-bearing sulfide ore sample (mainly chalcopyrite  
195 as example) are summarized as Eqs. (1) - (7). In the *A. ferrooxidans* system, the highest concentrations of  
196 ferrous ions in each system were (in mg/L) 200.5 (DF), 327.4 (UA) and 356.3 (AD). In the *A. thiooxidans*  
197 system, the values were (in mg/L) 65.4 (DF), 75.3 (UA) and 94.5 (AD). It was reported that the adsorption  
198 behavior of attached cells at the early stage is beneficial to further concentrate ferric ions and attack  
199 chalcopyrite, as shown Eq. (1).<sup>9,21</sup> The greatest increase in ferrous ions was 63.3%, which was tested in the  
200 *A. ferrooxidans*-DM system. It was owing to that the ferrous ion metabolism was more closely related with  
201 *A. ferrooxidans* than the pure sulfur oxidizer-*A. thiooxidans*. Furthermore, compared to reductive sulfur,  
202 ferrous ion was more easily utilized by *A. ferrooxidans* in a multiple-energies system.<sup>25,26</sup> The similar trend  
203 as ferrous ions was tested in ferric ions. In the *A. ferrooxidans* system, the highest concentrations of ferric  
204 ions in each system were (in mg/L) 435.2 (DF), 637.0 (UA) and 673.2 (AD). In *A. thiooxidans* system, the  
205 values were (in mg/L) 82.4 (DF), 123.2 (UA) and 137.8 (AD). These results indicated that the adapted  
206 evolution of adsorption behavior was favorable for enhancing iron metabolism.



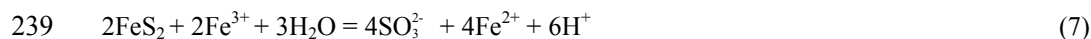
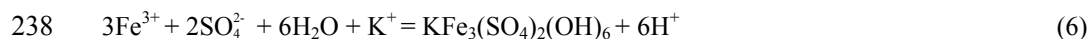
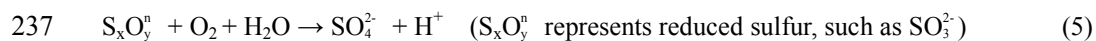
##### 210 3.1.2. Sulfur metabolism

#### 211 (Position for Fig. 1 and Table 3)

212 Similarly, the changes in pH and sulfate ion concentrations in different systems were also investigated  
213 (Fig. 1). After the adaptive phase, the pH gradually decreases along with the dissolution of the ore. In both  
214 the *A. ferrooxidans* and *A. thiooxidans* systems, the pH of the DM system was always the lowest, while the  
215 highest value was tested in DF systems. In the *A. ferrooxidans* system, the final pHs were 1.92 (DF), 1.82  
216 (UA), and 1.74 (AD). In the *A. thiooxidans* system, the final pHs were 1.82 (DF), 1.63 (UA), and 1.51

217 (AD). In the DF system, the granular sulfur on the ore surface could not be used by attached cells and thus  
 218 formed the S<sup>0</sup> passivation layer. The subsequent oxidization process was greatly inhibited. Conversely, in  
 219 the AD system, the adsorption behavior of attached cells was enhanced by the directionally domesticated  
 220 evolution. Most of the sulfur could be more efficiently utilized, as shown Eqs. (4) and (5), and produced  
 221 sulfuric acid. Moreover, the pH decline range of *A. thiooxidans* (1.82 to 1.51) was higher than that of *A.*  
 222 *ferrooxidans* (1.92 to 1.74), with the assistance of enhanced adsorption behavior.

223 Comparatively, the concentration of the sulfate ions steadily increased and achieved stability on day 20.  
 224 The trend of the sulfate ions in both *A. ferrooxidans* and *A. thiooxidans* systems was similar to the pH data.  
 225 In the *A. ferrooxidans* system, the highest concentrations of sulfate ions in each system were (in g/L) 2.93  
 226 (DF), 3.56 (UA) and 3.88 (AD). In the *A. thiooxidans* system, the highest concentrations of sulfate ions in  
 227 each system were (in g/L) 1.24 (DF), 2.83 (UA) and 3.86 g/L (AD). Compared to *A. ferrooxidans*-AD, the  
 228 increased range of sulfate ion concentration in the *A. thiooxidans*-AD system, via enhancing adsorption  
 229 behavior, was more significant. The dependence on the adsorption behavior with pure-sulfur oxidizer such  
 230 as *A. thiooxidans* was generally stronger, especially in eliminating S<sup>0</sup> membrane compared to  
 231 multiple-energies oxidizer.<sup>21</sup> It was also verified that the attached biomass of the *A. thiooxidans* system on  
 232 the sulfur surface was almost twice times of the *A. ferrooxidans* system.<sup>22</sup> The above result was also closely  
 233 consistent with the data on the changes in pH. These results all indicated the higher efficacy of adaptive  
 234 adsorption behavior on sulfur metabolism, especially for *A. thiooxidans*. The detailed comparison of key  
 235 chemical parameters in different systems is also listed in Table 3.



### 240 3.2. Effects of adaptive adsorption behavior on mineralogy

#### 241 3.2.1. Ore morphology

#### 242 (Position for Fig. 2)

243 To better understand the mineralogical effects of adapted adsorption behavior, the morphologies of ore

244 samples in different bioleaching systems were observed by SEM (Fig. 2). The morphological differences of  
245 between DF, UA, and AD systems were significant, from either *A. ferrooxidans* or *A. thiooxidans*. In the *A.*  
246 *ferrooxidans*-DF system, the ore surface was smooth and jarosite precipitation was tiny. Owing to the  
247 absence of attached cells, the “contact” mechanism was greatly inhibited and there was not enough energy  
248 substrate (ferrous ion) released from the ore for cell growth. The concentration of ferric ion sequentially  
249 decreased and further reduced jarosite production. In the *A. ferrooxidans*-UA system, more compact  
250 jarosite appeared on ore surface. With the assistance of adsorptive behavior, the iron metabolism was  
251 accelerated and produced more jarosite. In the *A. ferrooxidans*-AD system, the jarosite precipitation  
252 became significantly smaller and more potential adsorption sites were observed on the ore surface; jarosite  
253 formation was moderately inhibited by lower pH, as shown in Eq. (6), although with more active  
254 metabolism. The potential adsorption site indicated the stronger adsorption behavior via the adapted  
255 evolution.

256 The same phenomenon was more obvious in the *A. thiooxidans* system, to some extent. In the *A.*  
257 *thiooxidans*-DF system, the ore surface was smoother and the sulfur granule was extremely exiguous. In the  
258 *A. thiooxidans*-UA system, some rill and micro-pore appeared on the ore surface. In the *A. thiooxidans*-AD  
259 system, there were more sulfur granules and the ore surface was significantly rougher. Meanwhile, more  
260 potential adsorption sites indicated a stronger “contact” mechanism with adaptive attached cells. It was  
261 reported that the dependence on adsorption behavior with *A. thiooxidans* was stronger because most of the  
262 main energy source ( $S^0$ ) was generated on the ore surface.<sup>26</sup> Additionally, due to the active chemical ion  
263 status, more unknown derivatives were also generated and coupled with the ore.

### 264 3.2.2. Ore components

#### 265 (Position for Fig. 3)

266 The XRD analysis was performed to investigate the composition of ore samples in different bioleaching  
267 systems (Fig. 3). The main components were  $CuFeS_2$ ,  $KFe_3(SO_4)_2(OH)_6$ , S,  $Fe_7S_8$ ,  $Fe_3O_4$ ,  $FeS_2$  and  
268  $CaSO_4 \cdot 2H_2O$ . Compared to the *A. ferrooxidans*-DF system, there were fairly larger amounts of precipitate  
269 peaks with ore such as jarosite and granular sulfur in the UA system and especially the AD system. The  
270 higher activity of iron/sulfur metabolism was achieved by stronger adsorption behavior and further  
271 produced more crystal forms. The result was also closely consistent with the morphological differences

272 (Fig. 2). Compared to the *A. thiooxidans*-DF system, the sulfur peaks were more in the UA system,  
273 especially in the AD system, indicating that more crystal forms of elemental sulfur were generated with  
274 more active sulfur metabolism. It was reported that, to some extent, sulfur was generally coupled with  
275 amorphous iron or other oxy-hydroxides.<sup>18</sup> Meanwhile, the  $\text{CaSO}_4 \cdot 2\text{H}_2\text{O}$  peak was significant in the UA  
276 and AD systems, indicating higher concentration of sulfate ions. Additionally, minor accumulation of other  
277 unknown peak in these precipitates was due to previous washes with deionized water prior to XRD  
278 detection. It was also reported that the abundant inorganic ions and microbial organic compounds in  
279 bioleaching systems contribute to more complicated derivatives.<sup>20</sup>

### 280 3.3. Efficacy of adapted adsorption behavior for enhancing biomass and copper recovery

#### 281 3.3.1. Biomass

#### 282 (Position for Fig. 4)

283 With the assistance of adapted evolution, the attached biomass was significantly improved (Fig. 4A). In  
284 the *A. ferrooxidans* system, the highest attached biomass of each system was 0.62 (DF), 1.29 (UA) and 1.72  
285  $\times 10^7$  cells/mL (AD). The attached biomass was improved by 33.3% via the adapted evolution. Free  
286 biomass was also increased sequentially from 21.6 into 27.0  $\times 10^7$  cells/mL (25.0%); more energy and  
287 nutrients were released owing to a stronger “direct contact” mechanism. The phenomenon was more  
288 obvious in *A. thiooxidans* system. The highest attached biomass of each system was 0.81 (DF), 1.65 (UA)  
289 and 2.62  $\times 10^7$  cells/mL (AD). Attached biomass was improved by 58.9% via adapted evolution. Moreover,  
290 the free biomass increased from 11.8 to 15.8  $\times 10^7$  cells/mL (33.9%) with stronger adsorption behavior  
291 because *A. thiooxidans* is pure-energy oxidizer (sulfur), which is different from the multiple energy  
292 oxidizer-*A. ferrooxidans*. *A. thiooxidans* relied more on its attached cells because the main energy substrate  
293 ( $\text{S}^0$ ) largely existed on the ore surface. Sulfur granules were primarily oxidized into some intermediate  
294 status such as  $\text{S}_4\text{O}_6^{2-}$  or  $\text{S}_4\text{O}_5^{2-}$ , with the assistance of adsorption behavior. Then, the reduced and soluble  
295 sulfur was thoroughly utilized via a “non-contact” mechanism. These data are consistent with the TEM  
296 images of flagella and capsule, which also indicated a stronger requirement of attached cells by *A.*  
297 *thiooxidans* ZJJN-3.<sup>21</sup>

#### 298 3.3.2. Copper recovery

299 The copper recovery efficiency was significantly enhanced by the adaptive evolution of attached cells  
300 (Fig. 4B and Table 3). In the *A. ferrooxidans* system-AD, the efficiency was improved by 93.5% and 22.8%,  
301 compared to the DF and UA systems, respectively. The improvement in the *A. thiooxidans*-AD system was  
302 more significant. The efficiency was improved by 154.2% and 28.9%, compared to the DF and UA systems,  
303 respectively. In other words, more than 48.3%-60.7% of the bioleaching efficiency was contributed by  
304 directly domesticating attached cells. Compared to *A. ferrooxidans*, the efficacy of adaptive evolution was  
305 more prominent with *A. thiooxidans*. The result was also closely consistent with the chemical,  
306 mineralogical, and biological parameters, thereby proving the efficacy of adapted evolution.

307 *3.4. Overall assessment effects of adsorption behavior in bioleaching copper-bearing sulfide ore*

308 **(Position for Fig. 5 and Table 4)**

309 The microenvironments of bioleaching of copper-bearing sulfide ore were divided into solid-liquid  
310 and liquid microenvironments based on the biochemical reaction site (Fig. 5, chalcopyrite as example).  
311 Apparently, attached cells adsorbed onto ore surface in the solid-liquid microenvironment. The biochemical  
312 reaction in the liquid microenvironment was subsequently influenced by the surface adsorption process.  
313 The “direct contact” and “indirect contact” bioleaching mechanisms were derived from these two different  
314 microenvironments.<sup>25,27</sup> The role of attached biomass in bioleaching of copper-bearing sulfide ore was  
315 characterized by the aspects of iron and sulfur metabolisms.

316 In the “direct contact” mechanism’s iron metabolism (*A. ferrooxidans* CUMT-1), attached cells  
317 adsorbed onto the ore surface and oxidized ferrous ion into ferric ion, as shown in Eq. (3). The ore surface  
318 was sequentially attacked by generated ferric ion as Eq. (1) and dissolved copper ion. The resulting ferrous  
319 ion entered into the ion cycle again. The dissolution process of ore took place at the interface between the  
320 cells and the ore surface. Extracellular polymeric substance (EPS), consisting of some polysaccharides,  
321 proteins, and nucleic acids, generally served as the reaction space.<sup>28</sup> The increasing concentrations of  
322 ferrous and ferric ions in the liquid microenvironment gradually initiated and enhanced the “indirect  
323 contact” mechanism.<sup>29,30</sup> Also, the accumulated ferric ions partly participated during the formation of  
324 jarosite, as shown in Eq. (6).

325 In the “direct contact” mechanism’s sulfur metabolism (*A. thiooxidans* ZJJN-3/*A. ferrooxidans*

326 CUMT-1): in the “direct contact” mechanism, sulfur colloids were subsequently oxidized into intermediate  
327 compounds such as  $S_4O_6^{2-}$  or  $S_4O_5^{2-}$ . Also, redundant sulfur gathered as micro-particles ( $S_8$ ) and formed a  
328 passivation layer. This reduced sulfur dissolved into the liquid microenvironment and was oxidized, as  
329 shown in Eq. (5). Then, the hydrogen ions entered into the solid-liquid microenvironment and attacked ore  
330 surface, as shown in Eq. (2). The copper ion was finally released. Reduced sulfur and hydrogen ions in the  
331 liquid microenvironment gradually initiated and enhanced the “indirect contact” mechanism. With the  
332 assistance of adsorption behavior, more hydrogen ions, ferrous ions, ferric ions, sulfur compounds, and free  
333 biomass were created in the bioleaching system. The whole bioleaching system was directly or indirectly  
334 affected by these oxidizing and reductive agents. Therefore, in both iron and sulfur metabolism, adsorption  
335 behavior acted as an initiator and accelerator. Our research was the first time to reveal the enhancement  
336 mechanism coupling with adapted adsorption behavior from mineralogical aspect in bioleaching of  
337 copper-bearing sulfide ore.

#### 338 4. Conclusions

339 Bioleaching of copper-bearing sulfide ore was improved by directly adapting adsorption behavior, and  
340 its mineralogical enchantment mechanism was also successfully investigated and compared to DF and UA  
341 systems. With the assistance of adapted evolution, both iron and sulfur metabolism was greatly enhanced.  
342 Jarosite (*A. ferrooxidans*) and  $S^0$  (*A. thiooxidans*) became significantly smaller along with more potential  
343 adsorption sites. More compound derivatives were generated because of active biochemical reactions.  
344 Attached biomass was increased and further contributed to higher free biomass. Moreover, the efficiency of  
345 copper recovery was improved by 22.8% (*A. ferrooxidans*) and 28.9% (*A. thiooxidans*), respectively. Taken  
346 together, these results indicated that this mechanism can be applicable to directly domesticate adsorption  
347 behavior for improving bioleaching of copper-bearing sulfide ore, especially with *A. thiooxidans*.

#### 348 Acknowledgements

349 This work was supported by grants from the Natural Science Foundation of Jiangsu Province (No.  
350 BK20150133), the Scientific Program of Jiangnan University (No. JUSRP11538), the National Natural  
351 Science Foundation of China (Grant No. 31301540 and 21306064), the Priority Academic Program

352 Development of Jiangsu Higher Education Institutions, and the 111 Project (No. 111-2-06).

353 **References**

354 1 C. L. Zhu, L. Z. Liu, M. M. Fan, L. Liu, B. B. Dai, J. Z. Yang, D. P. Sun, *RSC Adv.*, 2014, 4,  
355 55044–55048.

356 2 S. K. Behera, P. P. Panda, S. Singh, N. Pradhan, L. B. Sukla, B. K. Mishra, *Int. Biodeter. Biodegr.*, 2011,  
357 65, 1035–1042.

358 3 D. B. Johnson, C. A. du Plessis, *Miner. Eng.*, 2015, 75, 2–5.

359 4 H. R. Watling, D. M. Collinson, J. Li, L. A. Mutch, F. A. Perrot, S. M. Rea, F. Reith, E. L. J. Watkin,  
360 *Miner. Eng.*, 2014, 56, 35–44.

361 5 M. Vera, A. Schippers, W. Sand, *Appl. Microbiol. Biotechnol.*, 2013, 97, 7529–7541.

362 6 S. Ghassa, Z. Boruomand, H. Abdollahi, M. Moradian, A. Akcil, *Sep. Purif. Technol.*, 2014, 136,  
363 241–249.

364 7 M. J. Chen, J. Q. Wang, J. X. Huang, H. Y. Chen, *RSC Adv.*, 2015, 5, 34921–24926.

365 8 S. O. Rastegar, S. M. Mousavi, S. A. Shojaosadati, *RSC Adv.*, 2015, 5, 41088–41097.

366 9 W. M. Zeng, G. Z. Qiu, H. Z. Zhou, J. H. Peng, M. Chen, S. N. Tan, W. L. Chao, X. D. Liu, Y. S. Zhang,  
367 *Bioresour. Technol.*, 2010, 101, 7068–7075.

368 10 J. Y. Zhu, Q. Li, W. F. Jiao, H. Jiang, W. Sand, J. L. Xia, X. D. Liu, W. Q. Qin, G. Z. Qiu, Y. H. Hua, L. Y.  
369 Chai, *Colloid. Surface. B.*, 2012, 94, 95–100.

370 11 H. R. Watling, *Hydrometallurgy*, 2006, 84, 81–108.

371 12 A. Schippers, W. Sand, *Appl. Environ. Microbiol.*, 1999, 65, 319–321.

372 13 F. K. Crundwell, *Hydrometallurgy*, 2003, 71, 75–81.

373 14 C.L. Brierley, J.A. Brierley, *Appl. Microbiol. Biotechnol.*, 2013, 97, 7543–7552.

374 15 N. Pradhan, K. C. Nathsarma, K. Srinivasa Rao, L. B. Sukla, B. K. Mishra, *Miner. Eng.*, 2008, 21,  
375 355–365.

376 16 S. N. Tan, M. Chen, *Hydrometallurgy*, 2012, 119–120, 87–94.

377 17 C. J. Africa, R. P. van Hille, S. T. L. Harrison, *Appl. Microbiol. Biotechnol.*, 2013, 97, 1317–1324.

378 18 S. Mangold, K. Harneit, T. Rohwerder, G. Claus, W. Sand, *Appl. Environ. Biotechnol.*, 2008, 74,

- 379 410–415.
- 380 19 K. Harneit, A. Göksel, D. Kock, J. H. Klock, T. Gehrke, W. Sand, *Hydrometallurgy*, 2006, 83,  
381 245–254.
- 382 20 M. A. Ghauri, N. Okibe, D. B. Johnson, *Hydrometallurgy*, 2007, 85, 72–80.
- 383 21 S. S. Feng, H. L. Yang, Y. Xin, L. Zhang, W. L. Kang, W. Wang, *J. Ind. Microbiol. Biotechnol.*, 2012,  
384 25–1635.
- 385 22 S. S. Feng, H. L. Yang, Y. Xin, L. K. Gao, J. W. Yang, T. Liu, L. Zhang, W. Wang, *Bioresour. Technol.*,  
386 2013, 129, 456–462.
- 387 23 S. S. Feng, H. L. Yang, X. Zhan, W. Wang, *Bioresour. Technol.*, 2014, 161, 371–378.
- 388 24 T. Gehrke, J. Telegdi, D. Thierry, W. Sand, *Appl. Environ. Biotechnol.*, 1998, 64, 2743–2747.
- 389 25 P. Devasia, K. A. Natarajan, *Int. J. Miner. Process.*, 2010, 94, 135–139.
- 390 26 P. Martínez, S. Gálvez, N. Ohtsuka, M. Budinich, M. P. Cortés, C. Serpell, K. Nakahigashi, A. Hirayama,  
391 M. Tomita, T. Soga, S. Martínez, A. Maass, P. Parada, *Metabolomics*, 2013, 9, 247–257.
- 392 27 R. H. Lara, J.V. García-Meza, R. Cruz, D. Valdez-Pérez, I. González, *Appl. Microbiol. Biotechnol.*,  
393 2012, 95, 799–809.
- 394 28 H. C. Flemming, J. Wingender, *Nat. Rev. Microbiol.*, 2010, 8, 623–633.
- 395 29 A. B. Vakylabad, M. Schaffie, M. Ranjbar, Z. Manafi, E. Darezereshki, *J. Hazard. Mater.*, 2012,  
396 241–242, 197–206.
- 397 30 L. Reyes-Bozo, M. Escudey, E. Vyhmeister, P. Higuera, A. Godoy-Faúndez, J. L. Salazar, H.  
398 Valdés-González, G. Wolf-Sepúlveda, R. Herrera-Urbina, *Miner. Eng.*, 2015, 78, 128–135.
- 399
- 400
- 401
- 402
- 403
- 404
- 405
- 406

407 **Table 1**

408 The main characteristics of strains used in the study.

Speices	Strain	Energy type	Optimal T/pH	Description and source
<i>A.ferrooxidans</i>	CUMT-1	Ferrous and sulfur oxidizer	30-35°C, pH 1.8-2.5	Waste acid mine drainge of coal ore, Jiangsu, China
<i>A.thiooxidans</i>	ZJJN-3	Sulfur oxidizer	28-30°C, pH 0-2.0	Leachate of Zijinshan Copper Mine, Fujian, China.

409

410

411

412

413

414

415

416

417

418

419

420

421

422

423

424

425

426

427

428

429

430

431

432

433 **Table 2**434 The main characteristics of ore sample used in the study<sup>a</sup>.

Parameter and unit	Value and description
Cu (%)	1.03 ± 0.05
S (%)	12.8 ± 0.21
Fe (%)	32.3 ± 0.53
Ca (%)	3.78 ± 0.32
Mg (%)	3.53 ± 0.25
Al (%)	1.66 ± 0.39
Zn (%)	0.051 ± 0.01
Mn (%)	0.044 ± 0.01
Ni (%)	0.029 ± 0.005
Pb (%)	0.028 ± 0.005
As (%)	0.0042 ± 0.001
Particle diameter (μm)	< 48 <sup>b</sup>

435 <sup>a</sup> The ore sample was collected from the Dongguashan copper mine, Tongling, Anhui, China; the values of  
 436 Ag, Au, Co, Cd and Hg were all below detection limitation (< 0.0002).

437 <sup>b</sup> The ore sample was ground and sieved through a 300-mesh grid, which controlled the particle diameter  
 438 <48 μm.  
 439

440

441

442

443

444

445

446

447

448

449

450

451

452

453

454

455

456 **Table 3**

457 Comparison of key chemical and biological parameters between pre-leaching and after-leaching in DF, UA  
 458 and AD systems.

	Parameter and unit	Pre-leaching	After-leaching					
			<i>A. ferrooxidans</i>			<i>A. thiooxidans</i>		
			DF	UA	AD	DF	UA	AD
Chem-indexes	pH	2.20	1.92	1.82	1.74	1.82	1.63	1.51
	ORP/mV	270	278	298	312	275	286	303
	Sulfate ion (g/L)	2.4/0.6	2.9	3.3	3.7	1.2	2.8	3.8
	Conversion ratio of sulfate ion % <sup>a</sup>	None	4.3	7.8	11.3	5.2	19.1	27.8
	Ferrous ion (mg/L)	None	162.5	312.5	356.3	65.4	75.3	94.5
	Conversion ratio of ferrous ion % <sup>a</sup>	None	1.7	3.2	3.7	0.7	0.8	1.0
	Ferric ion (mg/L)	None	432.2	564.5	675.3	82.0	123.2	137.8
	Conversion ratio of ferric ion % <sup>a</sup>	None	4.5	5.8	7.0	0.8	1.3	1.4
	Total iron (mg/L)	None	594.7	877.0	1031.6	147.4	198.5	232.3
	Conversion ratio of total iron % <sup>a</sup>	None	6.2	9.0	10.7	1.5	2.1	2.4
	Final copper ion (mg/L)	None	25.06	39.50	48.51	24.11	44.25	54.34
	Mineral color	Black	Tawny	Tawny	Tawny	Gray	Gray	Gray
	Mineral weight (g)	3.00	3.01	3.04	2.92	3.03	2.78	2.65
	Free biomass (10 <sup>7</sup> cells/mL)	5.0	17.9	21.6	27.0	8.3	11.8	15.8
Bio-indexes	Attached biomass (10 <sup>7</sup> cells/mL)	None	0.62	1.29	1.72	0.81	1.65	2.62
	Attached ratio (%)	None	3.34	5.97	6.37	8.90	12.27	14.22
	Total biomass (10 <sup>7</sup> cells/mL)	5.0	18.51	22.89	28.72	9.11	13.45	18.42
	Daily productivity (10 <sup>7</sup> cells/mL)	None	0.46	0.57	0.72	0.23	0.34	0.46

459 <sup>a</sup> It represents soluble ion (sulfate, ferrous, ferric, and total iron ion ) in bioleaching system.

**Figure captions**

**Fig. 1.** Changes in key chemical parameters in different bioleaching systems. (A): *A. ferrooxidans*-DF; (B): *A. ferrooxidans*-UA; (C): *A. ferrooxidans*-AD; (D) *A. thiooxidans*-DF; (E) *A. thiooxidans*-UA; (F) *A. thiooxidans*-AD. (■) pH; (▲) Ferrous ion; (□) Ferric ion; (△) Sulfate ion.

**Fig. 2.** Morphological surface differences of the ore samples between different bioleaching systems. (A): *A. ferrooxidans*-DF; (B): *A. ferrooxidans*-UA; (C): *A. ferrooxidans*-AD; (D) *A. thiooxidans*-DF; (E) *A. thiooxidans*-UA; (F) *A. thiooxidans*-AD.

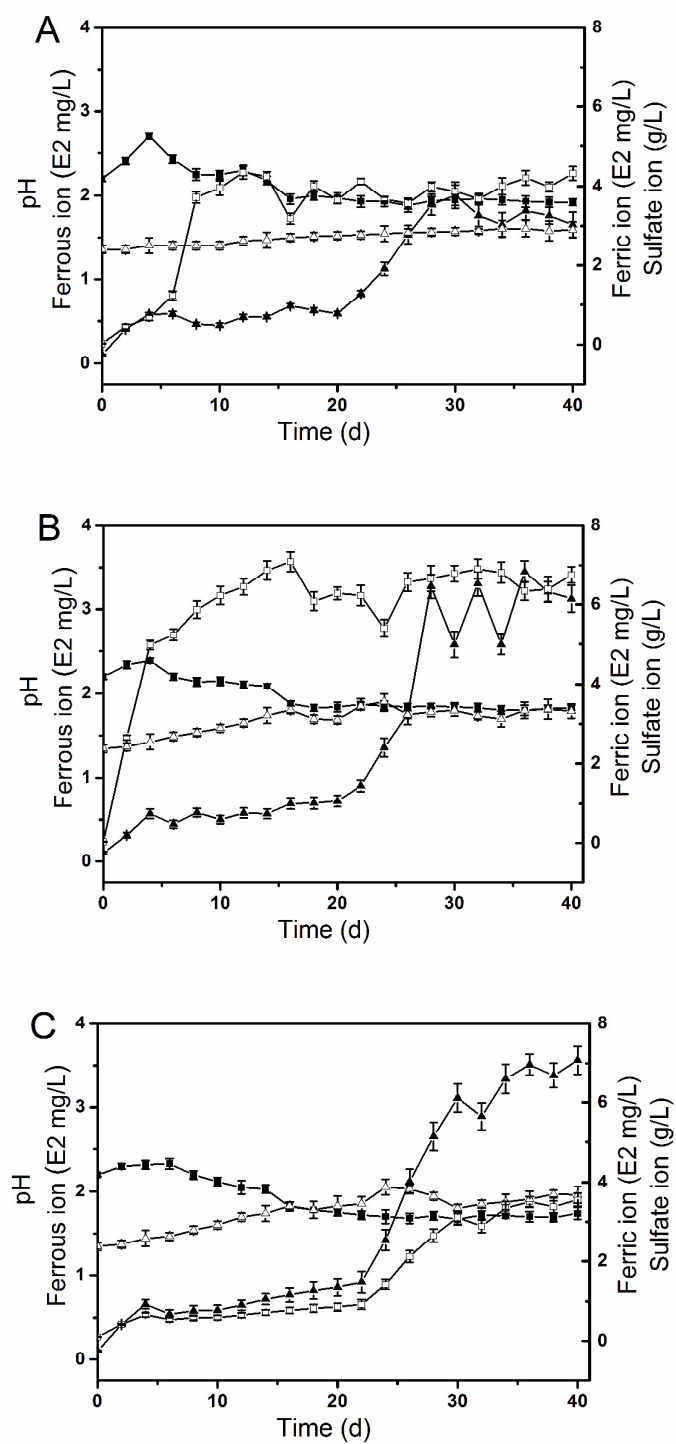
**Fig. 3.** XRD analysis of the ore samples in different bioleaching systems. (A): *A. ferrooxidans*-DF; (B): *A. ferrooxidans*-UA; (C): *A. ferrooxidans*-AD; (D) *A. thiooxidans*-DF; (E) *A. thiooxidans*-UA; (F) *A. thiooxidans*-AD. (■)  $\text{Fe}_3\text{O}_4$ ; (▲)  $\text{FeS}_2$ ; (●)  $\text{CuFeS}_2$ ; (□)  $\text{CaSO}_4 \cdot 2\text{H}_2\text{O}$ ; (△)  $\text{KFe}_3(\text{SO}_4)_2(\text{OH})_6$ ; (○)  $\text{Fe}_7\text{S}_8$  (★) S.

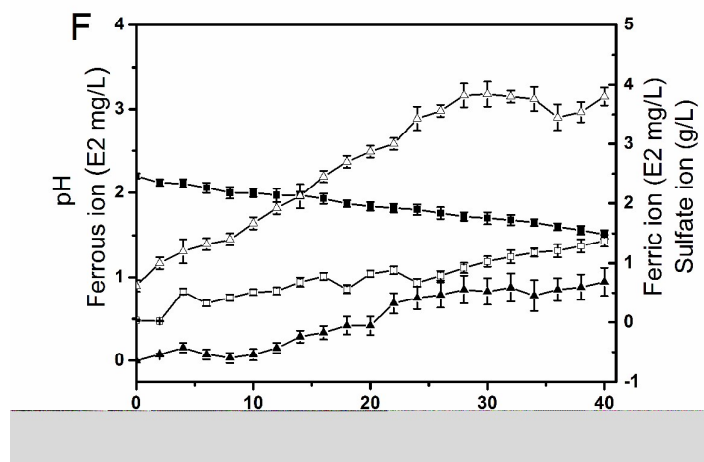
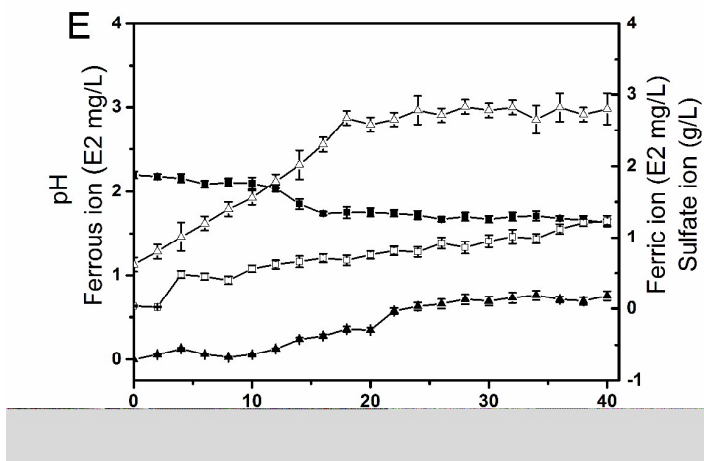
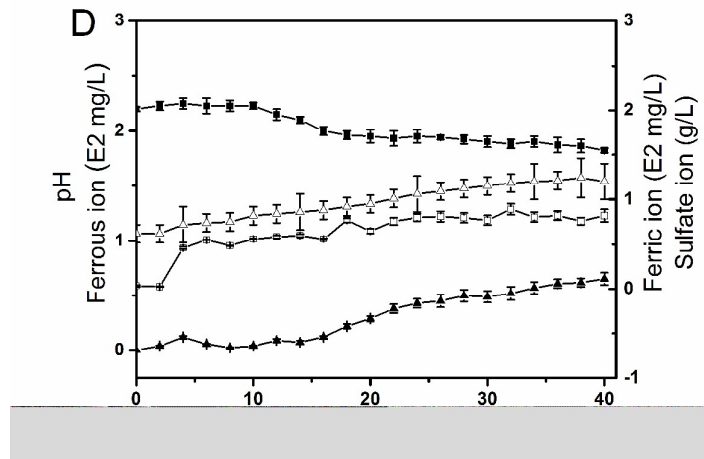
**Fig. 4.** The highest biomass and final recovery efficiencies of copper ion in different systems. (A) The highest free and attached biomass; (B) The final recovery efficiency of copper ion. a-c and A-C represent the statistically significant differences ( $c > b > a$ ;  $C > B > A$ ). The recovery efficiency of *A. ferrooxidans*-DF or *A. thiooxidans*-DF system was selected as the standard and defined as 100%. The relative recovery efficiency of *A. ferrooxidans*-DF/AD system and *A. thiooxidans*-DF/AD system was calculated by dividing the recovery efficiency of *A. ferrooxidans*-DF or *A. thiooxidans*-DF system.

**Fig. 5.** Overall effects of the adsorption behavior in bioleaching of copper-bearing sulfide ore (chalcopyrite as example).

Figures

Fig. 1.





RSC Advances Accepted Manuscript

Fig. 2.

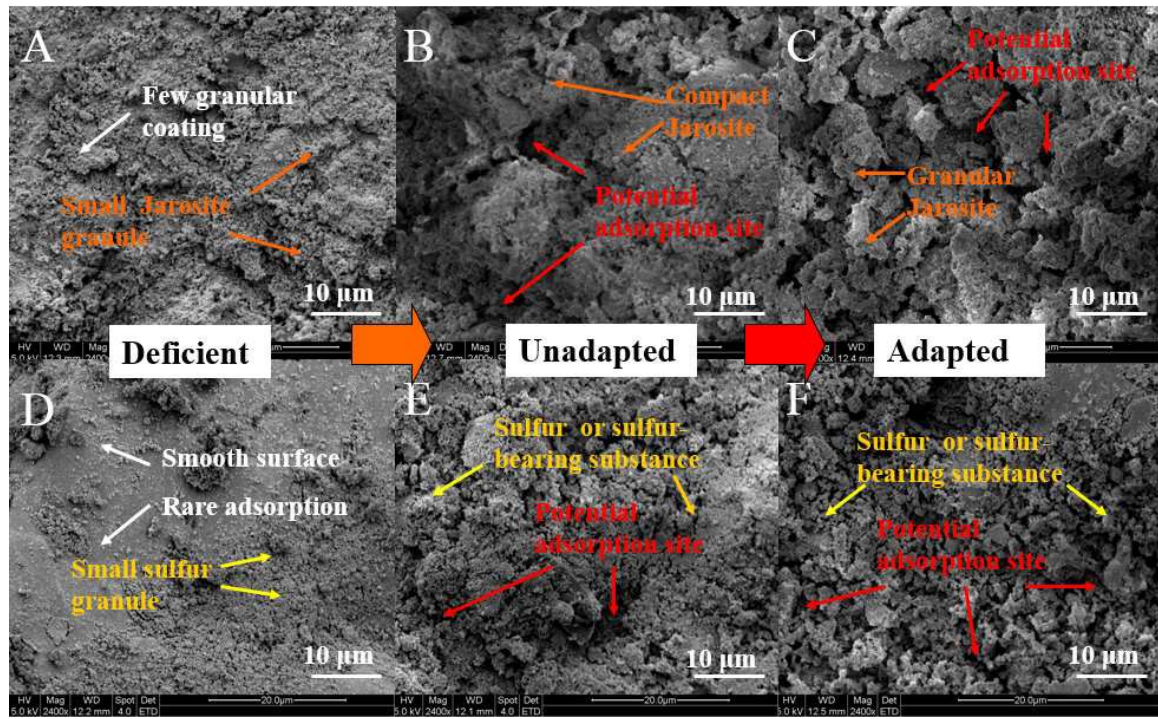
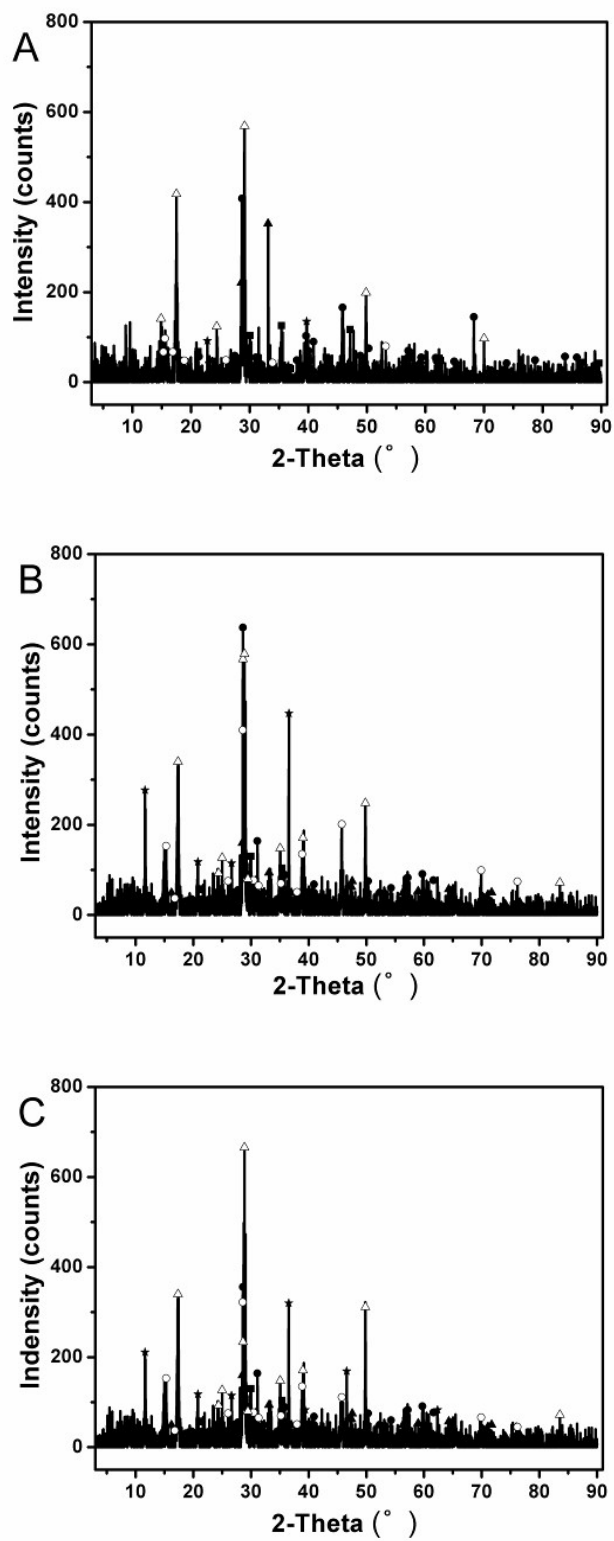


Fig. 3.



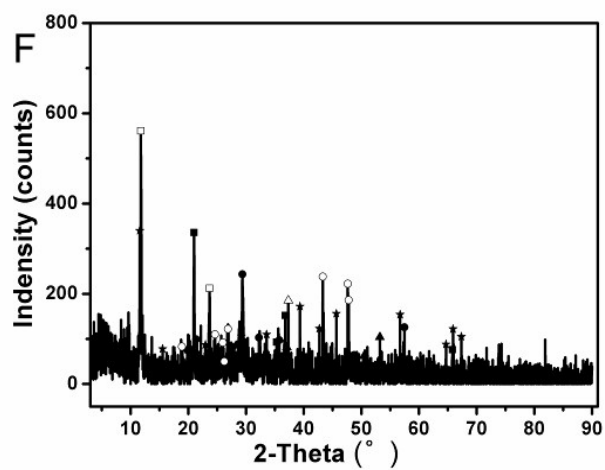
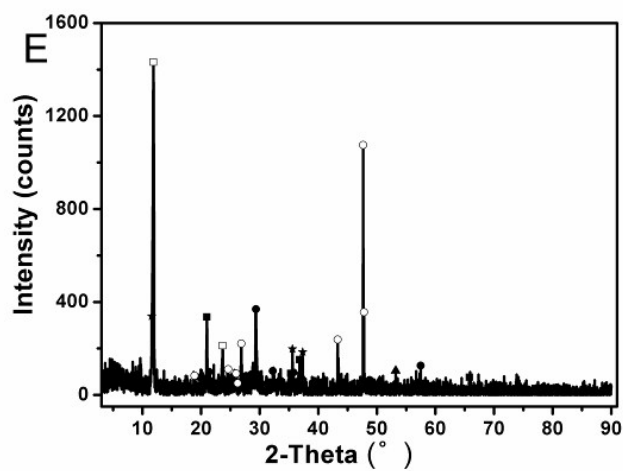
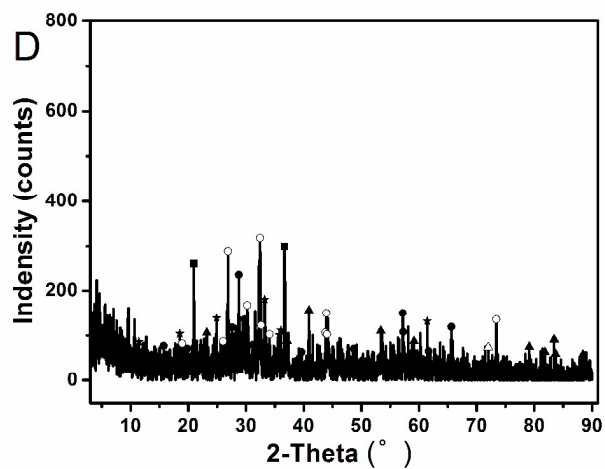


Fig. 4.

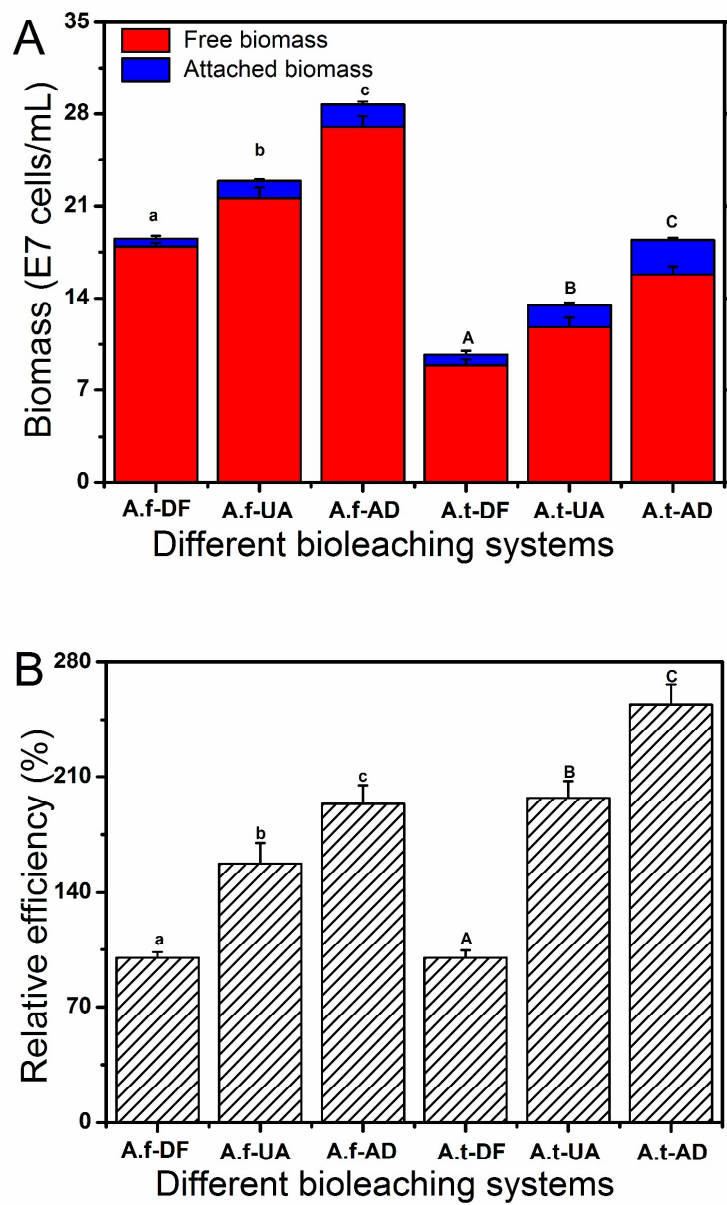


Fig. 5.

